Available online at www.sciencedirect.com
ScienceDirect
Microporous and Mesoporous Materials 95 (2006) 8–16
MICROPOROUS AND MESOPOROUS MATERIALS
www.elsevier.com/locate/micromeso

Claisen rearrangement of allyl phenyl ether over zeolites beta, mordenite and Y

S.G. Wagholikar, S. Mayadevi *, N.E. Jacob, S. Sivasanker

National Chemical Laboratory, Chemical Engineering and Process Development, Homi Bhabha Road, Pune 411008, India

Received 4 January 2006; received in revised form 28 April 2006; accepted 3 May 2006
Available online 19 June 2006

Abstract

The Claisen rearrangement of allyl phenyl ether (APE) to *o*-allylphenol was investigated over zeolites beta (BEA), mordenite (MOR) and Y (FAU) with different Si/Al ratios. Over the zeolite catalysts, the allylphenol cyclized to produce 2,3-dihydro-2-methyl benzofuran. Larger catalyst loading, higher reaction temperatures and longer run duration favored the formation of the ring compound. Conversion was small over MOR and FAU although they possessed higher acidity (as measured by the temperature programmed desorption of ammonia) compared to BEA. Studies using BEA revealed that the nature of the solvent influenced the reaction rate. The order of reactivity in the solvents was, benzene > EDC (1,2-dichloroethane) > toluene > TCE (1,1,2,2-tetrachloroethane) ≫ ACN (acetonitrile). The intermediate allylphenol reacted with the aromatic solvents to produce byproducts when benzene and toluene were used as solvents. A kinetic analysis assuming first order series and parallel reactions is presented.

Keywords: Claisen rearrangement; Allyl phenyl ether; Benzofuran; Allylphenol; Zeolites

1. Introduction

Claisen rearrangement of allyl phenyl ethers to the corresponding *o*-allylphenols normally takes place on heating the ethers (>473 K). Lewis and Brönsted acids, however, catalyze the reaction at lower temperatures [1,2]. The *o*-allylphenols undergo cyclization in the presence of acids to produce dihydrobenzofuran derivatives. Hence the reaction is an attractive route for the synthesis of benzofuran derivatives from substituted allyl aryl ethers. The rearrangement, when carried out with amino- and thio-derivatives, yields the corresponding heterocylic compounds.

Reports of the use of zeolitic materials as catalysts in Claisen rearrangement are limited. Pitchumani and co-workers have observed shape selectivity in ZSM-5 and ZSM-11 during their study of photo-assisted Claisen rearrangement [3,4]. The use of H-FAU and H-MOR in the rearrangement of APE in benzene medium [5,6] has also been studied. Other solid catalysts that have been investigated are mesoporous silica [7], bentonite [8] and Al-MCM-41 [9].

The present study is an extension of our earlier report on the use of wide pore zeolites (beta, mordenite and Y) as catalysts in the Claisen rearrangement of APE [10]. The earlier paper was centered mostly on the use of zeolite beta and it presented the effect of reaction conditions, the nature of the solvent and substrate structure on the reaction. Here, we present in detail the results of the Claisen rearrangement of APE over zeolites beta (BEA), mordenite (MOR) and Y (FAU). The effect of different zeolites, their aluminium content, acidity, reaction conditions, and solvents on conversion and product selectivity is discussed. A kinetic analysis of the formation of the different products under various reaction conditions is also presented. Tentative mechanisms for the reaction over acid sites leading to the major products are presented.

* Corresponding author. Tel.: +91 20 25902167; fax: +91 20 25893041.
E-mail address: s.mayadevi@ncl.res.in (S. Mayadevi).

1387-1811/$ - see front matter © 2006 Elsevier Inc. All rights reserved.
doi:10.1016/j.micromeso.2006.05.001

2. Experimental

2.1. Materials

H-beta (BEA(15); Si/Al = 15) and H-mordenite (MOR(11); Si/Al = 11) were obtained from PQ zeolites. Dealuminated samples of BEA and MOR were prepared from these parent zeolites. Zeolite beta was dealuminated by heating at 358 K with 55% (wt.) HNO_3 (60 g acid per g of zeolite) for 12 h. The dealuminated zeolite was repeatedly washed with deionised water and dried at 373 K. The procedure was repeated to obtain samples dealuminated to different extents. Mordenite samples with different Si/Al ratios were prepared by acid leaching (358 K) with 6 M hydrochloric acid for different time periods. The dealuminated samples were washed repeatedly with distilled water followed by dilute ammonia solution (1% solution) to remove residual acid and free aluminium species, and dried at 373 K for 2 h. Samples of faujasite (FAU) with Si/Al ratios 2.6, 15 and 40 were procured from Zeolyst, Holland. All the catalysts were calcined in air at 723 K for 6 h prior to use in the reactions.

Allyl phenyl ether was synthesized by allylation of phenol with allyl bromide and purified by standard methods. The purity of the prepared material was >98% as determined by GC analysis.

2.2. Characterization

The phase purity and crystallinity of the zeolites with different Si/Al ratios was analyzed by XRD (Rigaku, Miniflex). The total surface area of the samples was obtained from N_2 adsorption at liquid N_2 temperature by the BET method (Quantachrome, Nova 1200). As the BET method is not suitable for the use with zeolites, values for monolayer volume (V_m) were extracted from the initial section of the adsorption isotherms using the point-B method normally used in the case of Type-II isotherms that are typically obtained for micro- and meso-porous materials [11]. The external area of the samples was obtained by the *t*-plot method. Acidity of the zeolites was characterized by the TPD of NH_3 (Micromeritics, Autochem 2910). The standard procedure for TPD measurements involved the activation of the zeolite in flowing He at 873 K (3 h), cooling to 298 K and adsorbing NH_3 from a stream of He–NH_3 (10%), removing the physically adsorbed NH_3 by desorbing in He at 373 K for 1 h and finally carrying out the TPD experiment by raising the temperature of the catalyst in a programmed manner (10 K min^{-1}). The TPD curves were deconvoluted into two peaks and the areas under the peaks were converted into milliequivalents (meq) of NH_3 per gram of catalyst based on injection of known volumes of the He–NH_3 mixture at similar conditions. The ^{27}Al MAS NMR spectra of the samples were recorded on a Bruker (model, DRX-500) instrument. The spinning factor was 130.3 MHz, spinning speed was 10 kHz and pulse length was 10 s. The number of scans used approximated 1000.

2.3. Reactions

The reactions were carried out under N_2 in a two-necked round-bottomed flask (25 cm^3) equipped with a magnetic stirrer and a reflux (cold water) condenser. The flask was charged with the substrate (allyl ether; 1.25 mmol) and the solvent (3 g). Freshly calcined catalyst was added and the above mixture was stirred for 6 h at the required temperature. The progress of the reaction was monitored by withdrawing samples at different time intervals and analyzing them by gas chromatography (Varian; column: CP Sil 5CB, 30 m and i.d. 0.05 mm). The reaction products were identified by GC–MS and GC–IR.

2.4. Kinetics

The reaction of allyl phenyl ether over the catalysts produced the primary product, 2-allylphenol and the secondary product, 2-methyl-2,3-dihydrobenzofuran when it was carried out in an inert solvent like 1,2-dichloroethane (EDC) or 1,1,2,2-tetrachloroethane (TCE). However, when the reaction was carried out in reactive solvents like benzene or toluene, substantial amounts of side-products were formed (Fig. 1). These have been identified to be mainly the reaction (alkylation) products between the solvent and the intermediate allyl phenol.

The overall reaction may be represented as first order consecutive and parallel reactions as shown in Fig. 1. The constants of the first order series reaction k_1 and k_2 were obtained from the equations [9,10]

$$C_A/C_{A0} = e^{-k_1 t} \tag{1}$$

and

$$C_R/C_{A0} = k_1(e^{-k_1 t} - e^{-k_2 t})/(k_2 - k_1) \tag{2}$$

C_{A0} and C_A are the concentrations of APE at initial time, and at time t, respectively, C_R is the concentration of the intermediate product *o*-AP at time t, k_1 and k_2 are the rate constants for the first and second step, respectively. The values of k_2' and k_2'' in Fig. 1 were estimated from k_2 and the selectivity data.

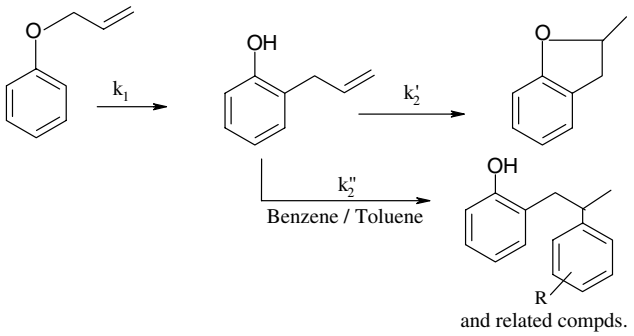

Fig. 1. Products of Claisen rearrangement of allyl phenyl ether over zeolite beta.

3. Results and discussion

3.1. Physicochemical characterization

The XRD patterns of all the dealuminated samples were similar to the parent sample. The crystallinity of the samples was not significantly affected by dealumination, the intensities of the prominent lines being within 10% of those of the parent sample. The total surface area, external surface area (by the *t*-plot method) and the pore volume of zeolites with different Si/Al ratios are given in Table 1. Surface areas of the samples were obtained by the BET and the point-B methods. The values obtained by the point-B method were slightly larger than those from the BET method, the difference being about 3.8% for BEA(15), 5.5% for MOR(11) and 6.3% for FAU(2.6). The external areas of the samples were obtained by the *t*-plot method. The external surface areas are derived from the external surface of the crystallites, mesopores in the crystallites and amorphous material. The external area of the beta samples are large, being ~17–25% of the total area. The external areas of the other zeolite samples are lower, contributing to about 6–10% of the total area. The small decrease in the external area on dealumination observed in the case of BEA may be due to the leaching out of amorphous material by the nitric acid. In the case of the other zeolites, the total area generally increased due to the formation of intracrystalline mesopores and crystal damage occurring during dealumination.

The TPD profiles of the zeolites (BEA, MOR and FAU) with different Si/Al ratios are presented in Fig. 2. The TPD profiles essentially consisted of two unresolved peaks for all the samples. These were deconvoluted into two distinct peaks with peak maxima in the range of 423–473 K for first peak and 623–823 K for the second peak. It is noticed (Fig. 2) that the temperature of the peak maximum for the strong acid centers decreases slightly on dealumination in the case of MOR and FAU. The decrease is about 20 K between MOR(11) and MOR(29) and between FAU(2.6) and FAU(6). The decrease becomes less significant on further dealumination. The reason for this observation is not clear though it is probable that the slight downward shift of temperature in the case of dealuminated samples is due to the greater ease of NH_3 desorption from the pores of the dealuminated samples. It was assumed that the two peaks represent NH_3 adsorbed from weak and strong acid sites. Based on this assumption and the amount of NH_3 desorbed, as obtained from the area under the corresponding peaks, strong and weak acidity (in meq/g) have been calculated and reported in Table 1. The number and density of acid sites in a given zeolite is expected to increase with its Al content. The table shows that the total number of acid sites and the strong and weak acid sites do increase with Al content for the three zeolites. However, the estimated acidity (strong and weak) is not directly proportional to the number of Al atoms present. The reasons are the presence of different amounts of the two types of Al-species (framework and non-framework) in the samples and the arbitrary nature of the classification of strong and weak acid centers based on the TPD profile. It is likely that, the rate of diffusion of NH_3 from acid sites at different locations (internal and inside the pores) is different and this could have an influence on the classification of the strong and weak acid centers based on the TPD profile. Hence, it should be noted that the data reported do not directly quantify any type of acidity, framework or otherwise and only serves to compare the relative acidity characteristics of the zeolites in a general way. The ^{27}Al MAS NMR spectra of the zeolites are presented in Fig. 3. It is seen from the spectra that all the commercial samples of the zeolites (BEA, MOR, FAU) contain O_h Al species (extra framework aluminium, EFAl). The framework species are observed in the samples at about 53–59 ppm and the O_h, (EFAl) species at about −1 ppm. On dealumination with acid, the EFAl decreases

Table 1
Physicochemical properties of the zeolite catalysts

Sample	Si/Al	Pore volume (cc/g)	Surface area (m^2/g)			Acidity (meq/g)	
			S_{BET}[a]	S_B[b]	External	Weak	Strong
Zeolite beta							
BEA(15)	15	0.32	656	681	166	0.55	0.67
BEA(34)	34	0.36	754	800	150	0.21	0.30
BEA(48)	48	0.35	760	795	128	0.09	0.30
Mordenite							
MOR(11)	11	0.24	562	593	52	0.82	1.05
MOR(29)	29	0.23	550	566	53	0.54	0.91
MOR(35)	35	0.22	519	551	35	0.47	0.84
MOR(57)	57	0.24	564	580	57	0.29	0.70
Faujasite (Zeolite Y)							
FAU(2.6)	2.6	0.33	795	848	48	0.89	1.34
FAU(6)	6	0.32	749	787	53	0.44	0.87
FAU(40)	40	0.34	747	782	77	0.06	0.2

[a] Obtained by BET method.
[b] Obtained by point-B method [11].

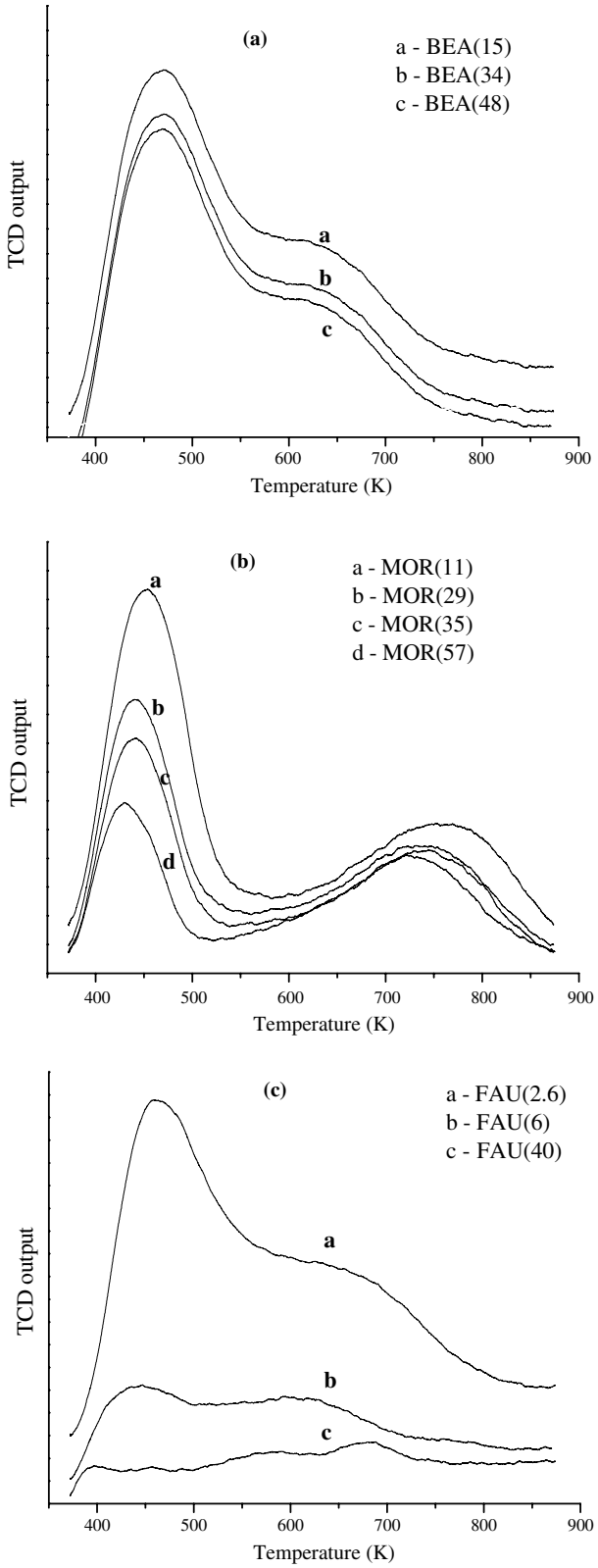

Fig. 2. Temperature programmed desorption profiles of ammonia from zeolites with different Si/Al ratios, (a) BEA, (b) MOR and (c) FAU.

in both BEA and MOR. In the case of FAU, all the samples were commercial Y samples and it is also found that the EFAl species decrease with increase in Si/Al ratio in these samples also.

3.2. Reaction studies

3.2.1. Claisen rearrangement of allyl phenyl ether

The catalytic activity of the calcined zeolites (BEA, MOR, FAU) with different Si/Al ratios has been investigated in the Claisen rearrangement of APE. The thermal reaction is reported to proceed through a series of two consecutive reactions [12]. The ether first undergoes rearrangement to produce allyl hexadienone followed by enolization to give *o*-AP which cyclizes to give 2,3-dihydro-2-methyl benzofuran (benzofuran). The intermediate allyl hexadienone could not be identified in any of the products in this study. Depending on the solvent used, side products (as shown in Fig. 1) were also formed in the reaction.

3.2.2. Influence of duration of run

The effect of run duration (up to 6 h) on *o*-allylphenol (*o*-AP) conversion and product selectivity for BEA(15), MOR(11) and FAU(2.6) (solvent, EDC) at 353 K are shown in Fig. 4(a)–(c). On BEA(15), the reaction proceeds rapidly up to about 75% conversion and slows down thereafter (Fig. 4(a)) as one would expect for a first order reaction. Similarly over FAU(2.6) also, the reaction proceeds rapidly initially though to a lower value of 25% and slows down thereafter. The slowing down of the reaction with time in this case could be due to both inherent first order kinetics and due to deactivation of the catalysts. In the case of MOR(11), however, the conversion increases slowly up to about 30% in about 6 h without any sign of deactivation due to strong adsorption of bulky products. It is likely that the initial rapid reaction over FAU(2.6) occurs at the external surface and inside the pores close to the external surface, and the rapid clogging of the pores slows down further reaction. In the case of MOR(11), presumably such pore blocking is not serious due to difficulty in formation of large molecules inside the smaller MOR pores. BEA(15) is the most active catalyst, even though the number of acid sites (both strong and weak) in MOR(11) and FAU(2.6) are larger than that in BEA(15). This may be due to the larger external surface area of BEA(15) that makes a larger number of active sites available for the reaction. *o*-AP appears to go through a maximum (as is expected for a consecutive reaction) in the case of BEA(15), although this is not clearly seen in Fig. 4(a) due to the absence of data at short run durations. In the case of MOR(11) and FAU(2.6), the observed trends for *o*-AP are consistent with its slow formation and destruction beyond 2 h.

3.2.3. Influence of catalyst weight

The influence of catalyst weight on conversion of APE and product selectivity for the reaction in TCE is presented in Fig. 5(a) (catalyst, BEA(15)). The nature of the conversion curve is similar to the reaction behavior with duration of run. It increases rapidly with increase in catalyst loading initially, but slows down at higher loadings due to the attainment of very high conversions. As the data has been

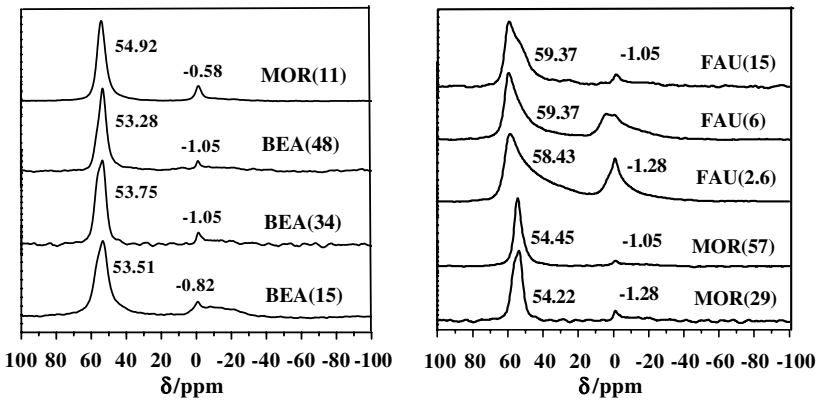

Fig. 3. ^{27}Al MAS NMR of BEA, MOR and FAU with different Si/Al ratios.

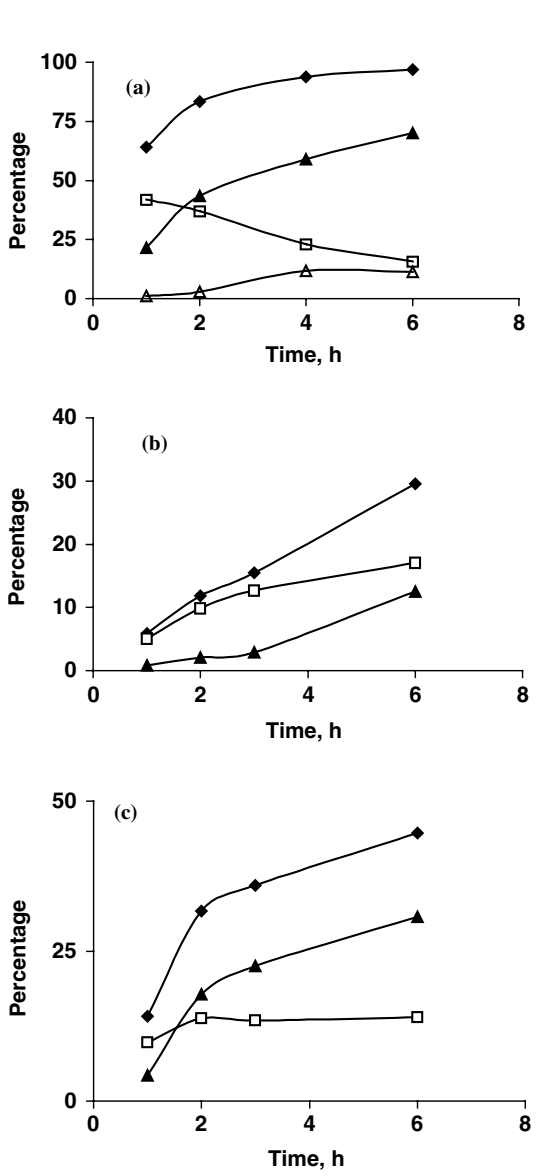

Fig. 4. Influence of duration of run on APE conversion and product yield (-♦-: conversion, -□-: *o*-AP, -▲-: furan, -△-: others) (temperature, 353 K; catalyst wt., 0.1 g; APE, 0.00125 mol; solvent, EDC; (a) BEA(15), (b) MOR(11), (c) FAU(2.6)).

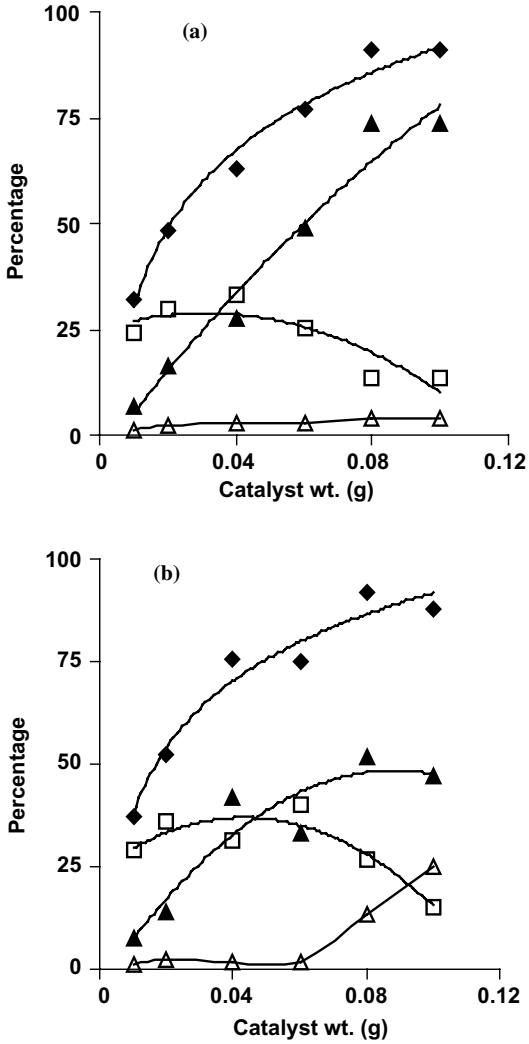

Fig. 5. Influence of catalyst weight on APE conversion and product yields over BEA(15). (-♦-: conversion, -□-: *o*-AP, -▲-: furan, -△-: others) (temperature, 353 K; APE, 0.00125 mol; reaction time, 3 h; (a) solvent TCE, (b) solvent toluene).

collected at a long run duration (3 h), the selectivity for *o*-AP decreases with catalyst weight, which is the typical behavior for the intermediate in a consecutive reaction.

Benzofuran selectivity and the side products formation increase with catalyst weight. In toluene, an increase in catalyst weight results in an increase in the side products formation at the expense of benzofuran (Fig. 5(b)). Toluene being a reactive solvent, the intermediate *o*-AP reacts with it to form the side products.

3.2.4. Influence of solvent

The solvent effect on the reaction of APE was studied over BEA(15) as it was the most active catalyst among the zeolites. The reaction of APE over BEA(15) produced both the primary product, 2-allylphenol (*o*-AP) and the secondary product, 2-methyl-2,3-dihydrobenzofuran when it was carried out in an inert solvent like EDC or TCE. The reaction did not proceed at all in dimethylformamide (DMF). However, when the reaction was carried out in reactive solvents like benzene or toluene, substantial amounts of side-products were formed. The side products formed in benzene and toluene have been identified to be mainly the reaction (alkylation) products between the solvent and the intermediate allyl phenol (Fig. 1). The nature of the solvent was found to affect the reaction rate. The order of reactivity in the solvents was benzene > EDC > toluene > TCE ≫ ACN (acetonitrile) (Table 2). In ACN, the reaction stopped at the first step with 100% selectivity for *o*-AP (conversion: 7.5% at the end of 6 h). The selectivity for benzofuran was most in TCE due to the near absence of by-products (Table 2).

The influence of the solvent on zeolite-catalyzed reactions can be complex. The solvent may affect the reactivity of the reaction intermediate, it may also adsorb strongly and poison the active sites, cause substrate exclusion from the surface due to strong adsorption effects and increase the resistance to diffusion of the reactants and the substrates inside the channels. In the case of the solvents used, all except ACN and DMF had low polarities (dielectric constants between 2.2 and 2.4 at 293 K). The reason for the low to negligible activity observed in DMF and ACN may be primarily due to their strong adsorption owing to their large dielectric constant (37.6 and 37.5, respectively) and excluding the substrate molecules from the active centres.

3.2.5. Influence of aluminium content

Negligible reaction occurred in the absence of a catalyst and when a purely siliceous, high surface area material (MCM-41) was used as the catalyst, even at 373 K [10]. This suggests that the reaction is catalyzed by the acid centers on zeolites. Very surprisingly, both conversion and selectivity in the Claisen rearrangement are found to be inversely dependent on the Al content of BEA, MOR and FAU as can be seen from Fig. 6. As the Al content of the zeolite decreases (increase in the Si/Al ratio), the strong and weak acidity decrease. However, the APE conversion is more over the dealuminated catalysts. Dealumination by steaming and acid leaching methods is known to create mesopores in zeolite crystals giving the reactant greater access to the acid centers. A recent discussion of the mesopore formation in zeolites during dealumination may be found in Ref. [13].

Table 2
Effect of different solvents on APE conversion and selectivity (catalyst: BEA(15), reaction time: 3 h, temperature: 353 K)

Solvent	Conversion of APE	Selectivity (%)		
		o-AP	Benzofuran	Side products
EDC	91.7	29.1	56.6	14.3
TCE	90.8	14.9	80.9	3.8
Toluene	88.0	17.5	53.5	28.6
Benzene[a]	95.9	3.1	67.2	29.7
ACN[a]	3.2	100	–	–

[a] Reaction time: 2 h.

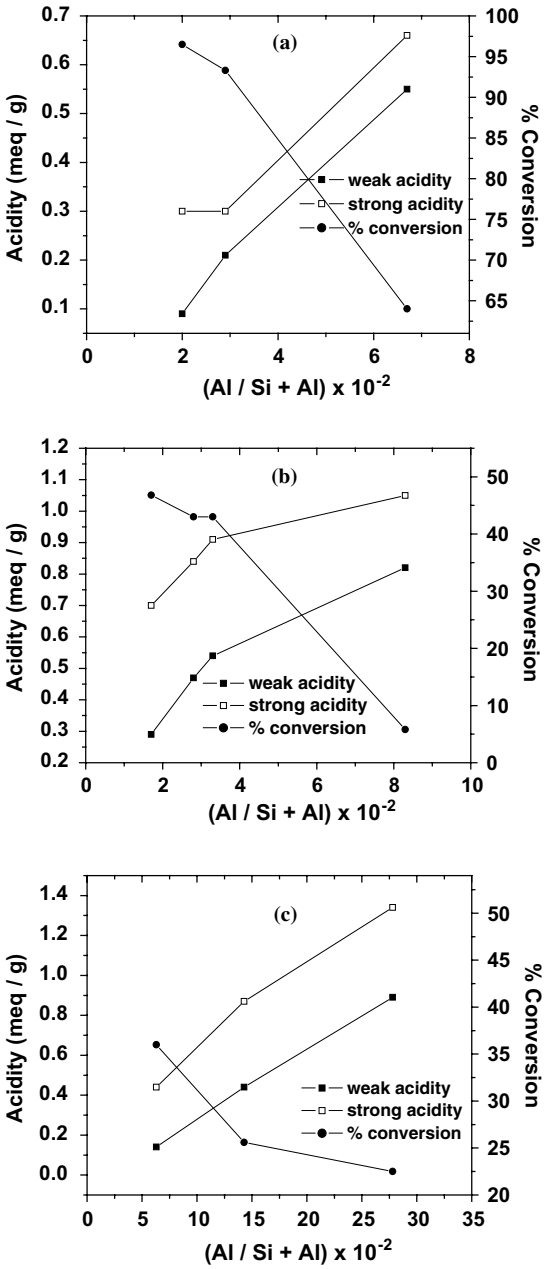

Fig. 6. Influence of Al-content of zeolites on (a) acidity and APE conversion (reaction time, 2 h; temperature, 353 K; catalyst wt., 0.1 g; APE, 0.00125 mol; solvent EDC; (a) BEA, (b) MOR, (c) FAU).

In general, dealumination increases the diffusivity of the reactants and products. It appears therefore that the reaction occurs mainly on the external surface of the zeolite crystallites and inside the pores close to the external surface, and dealumination enhances the accessibility of the acid sites to the reactant molecules by creating a mesoporous system in the crystallites, thus enhancing the accessibility of the acid centers, thereby increasing the productivity of the Al-ions. Thus, the positive effect of increased diffusion of the molecules greatly offsets the decrease in the number of acid centers. This is clearly seen in Fig. 7 wherein the TOF (moles converted per mole of Al per hour) is plotted against Al content. Al-ions in the dealuminated samples are found to be catalytically more effective. Another explanation for the observation of increasing activity on dealumination may be the creation of additional Lewis acid sites (mostly EFAl species) that are very active for the reaction during the dealumination process. Earlier workers have reported the formation of Lewis acid sites during the steam dealumination of FAU and also reported increased conversions with dealumination during their studies on anisole acylation [14,15]. Presumably, the source of these Lewis acid sites was the extraframework Al created during thermal dealumination. In our case, Al NMR studies reveal that the acid dealumination method had actually decreased the EFAl (O_h species) in BEA and MOR. In the case of FAU (commercial samples) also, the amount of EFAl decreased with increasing Si/Al ratio (Fig. 3). It appears, therefore,

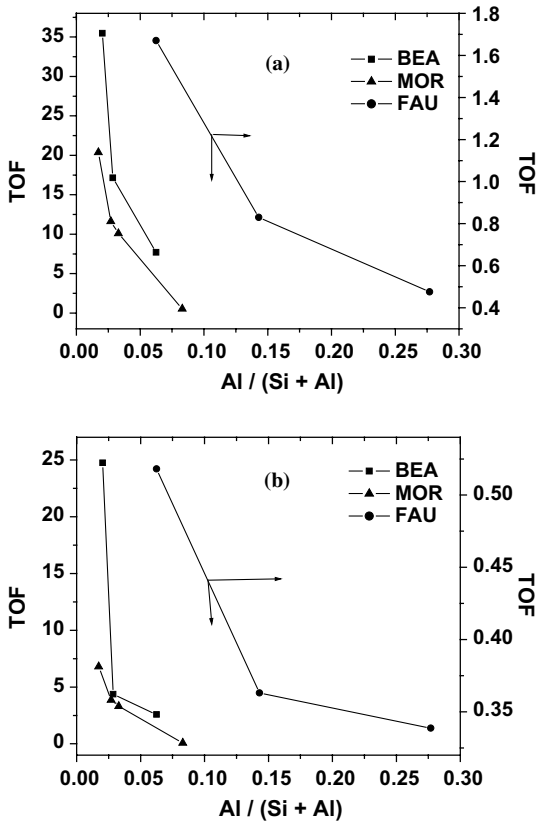

Fig. 7. Influence of Al-content of zeolites on turnover frequencies (TOF) for (a) conversion of APE and (b) formation of benzofuran (reaction time, 2 h; temperature, 353 K; catalyst wt., 0.1 g; APE, 0.00125 mol; solvent, EDC).

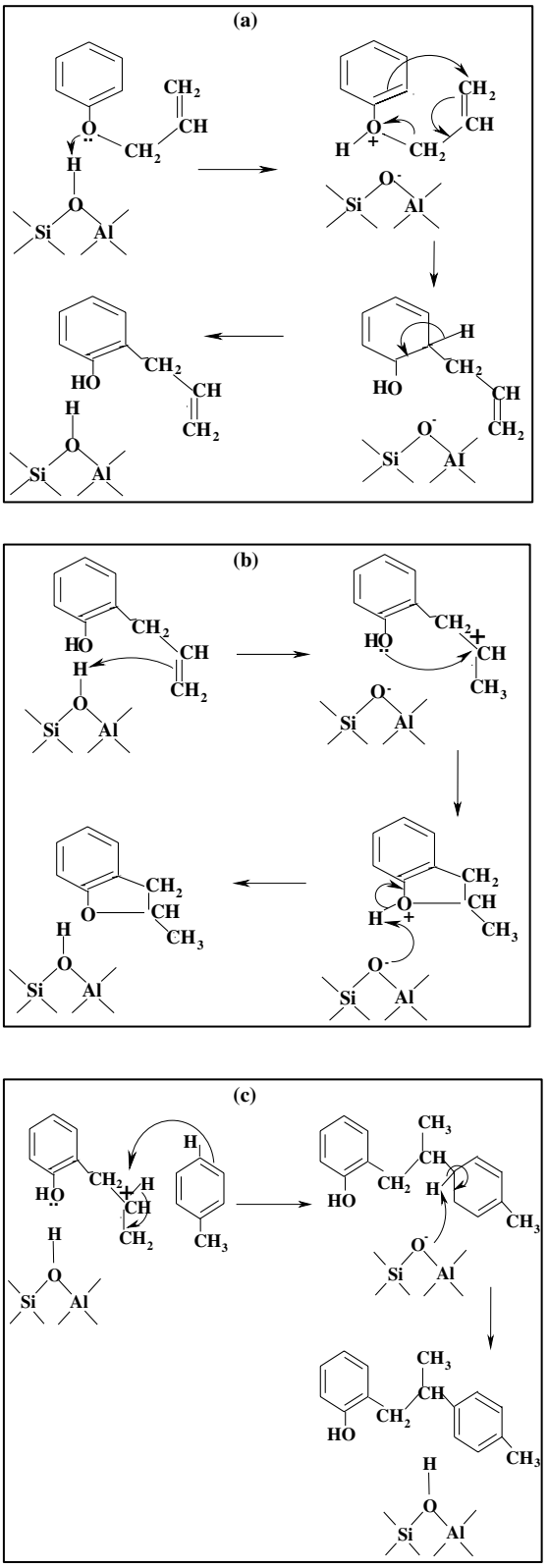

Fig. 8. Plausible mechanism of Claisen rearrangement of APE over zeolites, (a) for the formation of AP, (b) for the formation of ring product and (c) for the formation of byproducts.

that the creation of new Lewis acid sites is not a possible explanation for our observations.

3.2.6. Mechanism of the reactions

Plausible mechanisms for the initial Claisen rearrangement to produce the allyl phenol and the subsequent conversion of the phenol into the ring compound or byproducts are presented in Fig. 8(a)–(c). The steps are catalyzed by acid centers as discussed in our earlier study on Al-MCM-41 [9]. In the first step, namely the formation of the intermediate allylphenol (a), the acid site protonates the –O– of the ether to form the phenol. This is followed by intramolecular rearrangement of the protonated (adsorbed) species into the *o*-allyl phenol as shown in Fig. 8(a) [9]. The allyl phenol is next protonated at the allylic double bond to produce the secondary carbenium ion that reacts again intramolecularly with the phenolic 'O' to produce the benzofuran (Fig. 8(b)) [9]. When the reaction is carried out in the presence of the aromatic solvents benzene or toluene, an electrophilic attack of the carbenium ion takes place on the aromatic ring to produce the byproducts (Fig. 8(c)).

3.3. Kinetic analysis

Typical plots for two cases comparing the experimental data with those derived from the kinetic model (first order consecutive and parallel reaction) for the reaction in toluene and in tetrachloroethane (TCE) are presented in Fig. 9(a) and (b) respectively. In the figure, the lines represent compositions based on the kinetic equation. The symbols represent the concentration of individual components relative to the initial concentration of APE. It can be seen that the kinetic predictions are in good agreement with the experimental data confirming first order consecutive and parallel reaction kinetics.

The rate constants of the various steps over BEA(15) for different temperatures and solvents (toluene and TCE) are presented in Table 3. The rate constants were derived assuming a consecutive first order reaction. The rate constants for the disappearance of the substrate (APE) is k_1, while k_2' and k_2'' are the rate constants for the formation of the benzofuran derivative and side-products, respectively. It is noticed from the table that the reaction is much faster (k_1 values are larger) in toluene than in TCE at 363 and 383 K. On the other hand, k_2' is of similar magnitude in both the solvents (at a given temperature) suggesting a similar activity of the catalyst for ring product formation in both the solvents. The formation of side-products (k_2'') as already mentioned is substantial in toluene and negligible in TCE. The apparent activation energies (E_a) calculated for the different steps are also presented in Table 3.

The influence of aluminium content on the reaction kinetics in EDC over the catalysts BEA, MOR and FAU are presented as a plot of the rate constants (after

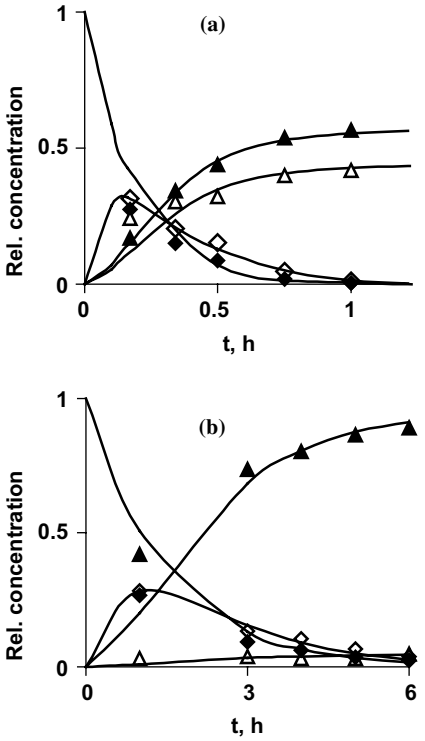

Fig. 9. A comparison between model (first order consecutive and parallel reaction kinetics) and measured data for the reaction (catalyst, BEA(15), 0.1 g; APE, 0.00125 mol). The symbols (-♦-: APE, -◇-: AP, -▲-: benzofuran, -△-: side products) represent experimental concentrations relative to the initial concentration of the reactant. (a) Solvent: toluene, temperature: 373 K; (b) solvent: TCE, temperature: 353 K.

Table 3
Effect of different solvents on the rate constant and activation energy (substrate: APE; catalyst: BEA(15))

Solvent	Temperature (K)	Rate constant (1/h) for		
		Depletion of APE (k_1)	Formation of furan (k_2')	Formation of side product (k_2'')
Toluene	343	0.11	0.08	0.07
	363	5.65	0.37	0.49
	383	11.43	0.94	1.44
	Activation energy (kcal/mol)	30.0	12.9	20.8
TCE	343	0.19	0.24	0.02
	363	0.74	0.33	–
	383	3.69	0.89	–
	Activation energy (kcal/mol)	18.2	14.1	–

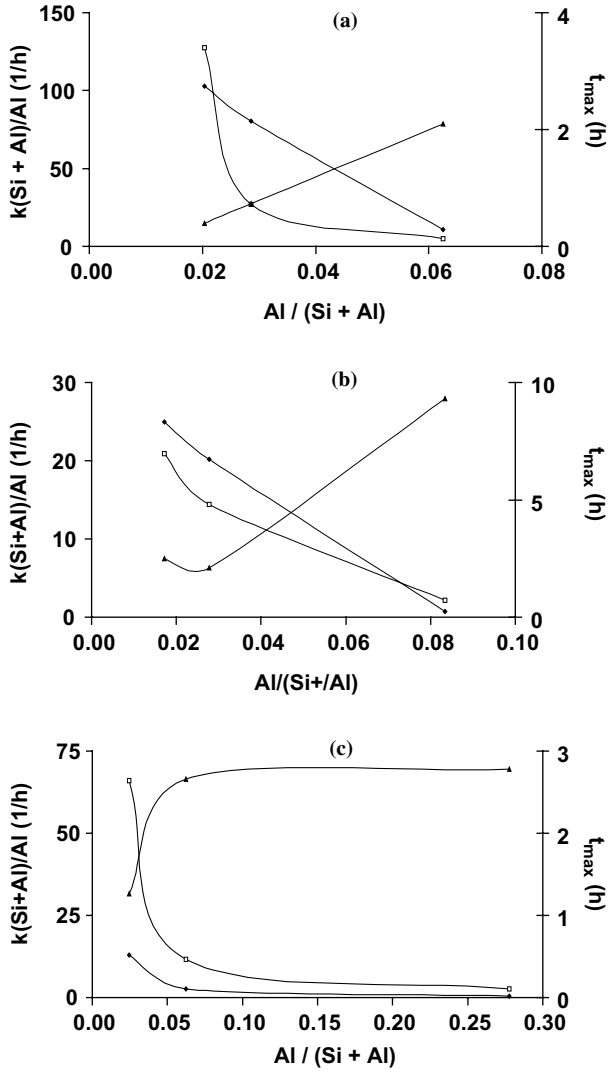

Fig. 10. Influence of Al-content on the rate constants of the two steps and time for maximum concentration of *o*-AP in the Claisen rearrangement of APE over zeolites. (-♦-: k_1, -□-: k_2, -▲-: t_{max}) (solvent, EDC; temperature, 353 K; (a) BEA(15), (b) MOR(11), (c) FAU(2.6)).

normalizing for Al-content) versus Al-content of the zeolites for the two reaction steps, in Fig. 10(a)–(c). The figures show that the conversion of APE and the formation of benzofuran are both sensitive to the Al-content, and the sensitivity depends on the zeolite type. The general trend of the normalized k_1 and k_2 values decreasing with Al-content is similar to the trend already reported for TOF (Fig. 7). Corresponding to this, t_{max}, the time at which the concentration of the intermediate product is maximum, also increases steadily. The sensitivity of the reactions for change in Al-content is different for BEA, MOR and FAU even though the trends are similar.

4. Conclusions

The Claisen rearrangement of allyl aryl phenol occurs rapidly over the large pore zeolites, BEA, MOR and FAU even at temperatures as low as 353 K. The initial products formed (*o*-allylphenols) cyclize readily into benzofuran derivatives. An increase in the temperature of the reaction or the amount of catalyst increases the formation of the ring product. The reaction proceeds rapidly both in inert solvents such as EDC and TCE, and in reactive solvents such as benzene and toluene. In the latter solvents, the intermediate allylphenol reacts with the solvent to produce byproducts. The acidity of the zeolites, measured by the TPD of ammonia, decreases progressively on increasing levels of dealumination with nitric acid. However, the activity of the catalyst increases with increasing dealumination and decreasing number of acid sites. This is attributed to the reaction occurring mainly inside the pores close to the external pore-openings and at the external surface of the zeolite crystallites, and dealumination increasing the accessibility of the acid centers to the reactant molecules through creation of mesopores. The conversion is poor over MOR and FAU despite having higher acidity compared to BEA. This may be due to their low external surface areas. A kinetic analysis reveals that the reaction follows typical first order consecutive and parallel reaction kinetics. The rate constants for the different zeolites derived from the kinetic analysis enable a better understanding of the activity of the different substrates. Plausible mechanisms for the different reaction steps based on acid catalysis have been proposed.

References

[1] J. March, Advanced Organic Chemistry, fourth ed., Wiley, New York, 1992.
[2] R.P. Lutz, Chem. Rev. 84 (1984) 205.
[3] K. Pitchumani, M. Warrier, V. Ramamurthy, Res. Chem. Intermediates 25 (1999) 623.
[4] K. Pitchumani, M. Warrier, V. Ramamurthy, J. Am. Chem. Soc. 118 (1996) 9428.
[5] J.A. Elings, R.S. Downing, R.A. Sheldon, Stud. Surf. Sci. Catal. 94 (1995) 487.
[6] R.A. Sheldon, J.A. Elings, S.K. Lee, H.E.B. Lempers, R.S. Downing, J. Mol. Catal. A: Chem. 134 (1998) 129.
[7] I. Sucholeiki, M.R. Pavia, C.T. Kresge, S.B. McCullen, A. Malek, S. Schram, Mol. Diversity 3 (1998) 151, CA: 129 (1999) 202736.
[8] R. Cruz-Almanza, F. Perez-Flores, L. Brena, E. Tapia, R. Ojeda, A.J. Fuentes, Heterocycl. Chem. 32 (1995) 219.
[9] N.T. Mathew, S. Khaire, S. Mayadevi, R. Jha, S. Sivasanker, J. Catal. 229 (2005) 105.
[10] S.G. Wagholikar, S.P. Mirajkar, S. Mayadevi, S. Sivasanker, in: E. van Steen, L. Callanan, M. Claeys, C.T. O' Conner (Eds.), Proc. 14th Int. Zeol. Conf., Cape Town, 25–30 April 2004, p. 2731.
[11] S.J. Gregg, K.S.W. Sing, Adsorption, Surface Area and Porosity, Academic Press, 1967, p. 54 (Chapter 2).
[12] V.G.S. Box, P.C. Meleties, Heterocycles 48 (10) (1998) 2173.
[13] H. van Bekkum, E.M. Flanigen, P.A. Jacobs, J.C. Jansen (Eds.), Introduction to Zeolite Science and Practice, second ed., Elsevier, Amsterdam, 2001.
[14] Y. Ma, Q.L. Wang, W. Jiang, B. Zuo, Appl. Catal. A: Gen. 165 (1997) 199.
[15] U. Freese, F. Heinrich, F. Roessner, Catal. Today 49 (1999) 237.